RSC Advances




ROYAL SOCIETY OF CHEMISTRY

www.rsc.org/advances

Cite this: DOI: 10.1039/c0xx00000x

www.rsc.org/xxxxxx

ARTICLE TYPE

# The dissolution behaviour of chitosan in acetate-based ionic liquids and their interactions: from experimental evidence to density functional theory analysis

**Xiaofu Sun,[a] Qingqing Tian,[b] Zhimin Xue,[a] Yuwei Zhang[a] and Tiancheng Mu*[a]**

***Received (in XXX, XXX) Xth XXXXXXXXX 20XX, Accepted Xth XXXXXXXXX 20XX***
**DOI: 10.1039/b000000x**

The searches for sustainable solvents of chitosan have drawn widely attention in recent years. In this study, nine acetate-based ionic liquids (ILs) varying in cation are used to explore the dissolution behavior of chitosan and the interactions between IL and chitosan. The solubilities of chitosan in these ILs have been determined in the temperature range from 40 °C to 140 °C with 10 °C intervals. For the imidazolium-based ILs, the solution thermodynamic parameters of chitosan have been calculated from the solubility data. The effects of cation type, alkyl chain structure, temperature and water content on the dissolution were investigated. Hydrogen bond donating and accepting abilities of ILs have been estimated by $^{1}$H nuclear magnetic resonance (NMR) spectroscopy and solvatochromic ultraviolet-visible (UV-vis) spectroscopy probe measurements. Temperature dependence of $^{13}$C NMR spectra and density functional theory (DFT) computations show that both cations and $OAc^-$ anion of ILs play significant roles in the chitosan dissolution process by the disruption of inherent hydrogen bonds of chitosan. And the interchain hydrogen bonds may be disrupted prior to the intrachain hydrogen bonds in the process of chitosan dissolution. In addition, low ionicity and special hydrogen bond interactions are used to explain the low chitosan solubility in the four quaternary ammonium-based ILs.

## Introduction

As the increasing shortage of the non-renewable fossil fuel, new and sustainable energy or materials are under developing to reduce the dependence on the oil, coal and other traditional energy resources.[1] Chitin is a ubiquitous polysaccharide and the second most abundant biopolymer after cellulose in nature.[2] Resembling the structure of cellulose, chitosan - the acetylated counterpart chitin - is not only composed of D-glucosamine units linked by β-(1,4) glucosidic bonds,[3] but also of N-acetylated D-glucosamine units in variable proportions, which can be specified by the degree of deacetylation. The excellent properties such as low toxicity, biocompatibility and antimicrobial activity make chitosan useful for fertilizer, membrane separation, ion-exchange resins, pharmaceutics, cosmetics and so on.[4-7] Unfortunately, due to the close packing by the intra- and inter-molecular hydrogen bonds, chitosan is extremely difficult to dissolve in most of the conventional organic solvents, which is the main obstacle for the further application of chitosan. Since the middle period of 20th century, various systems such as the aqueous solutions of some inorganic acids and hexafluoro-2-propanol have been developed for chitosan dissolution,[3, 8-10] but those systems have drawbacks more or less in high viscosity and the acidic aqueous medium, which is unsuitable for some reactions with chitosan. Besides, the higher concentrated acids are corrosive and toxicity. At the same time, difficulty in solvent recovery is another limit in dissolution process. Consequently, it is highly desirable to seek effective and sustainable solvents for chitosan dissolution.

Ionic liquids (ILs), are defined as organic molten salts, composed of ions, and generally are liquid below 100°C.[11-12] ILs have many unique physical and chemical properties such as low melting point, negligible vapour pressure, wide liquid range, excellent thermal stability, outstanding solvation potential, non-flammability, and wide electrochemical window, which make them be classified as "green solvents". Many researchers have begun to explore known chemical reactions and processes using ILs to replace the conventional organic solvents.[13-15] In addition, the properties of ILs can be easily tuned by varying the cation or anion, which expands their applications to organic synthesis,[16] catalytic reactions,[17-19] life science,[20] functional materials,[21] clean energy,[22] and so on. Since Swatloski*et al.*[23] reported that cellulose could be efficiently dissolved in ILs for the first time, an ever-increasingly number of researchers have focused on the dissolution of biomass using ILs.[24-30] Due to the analogous structures for chitosan and cellulose, previous studies on chitosan dissolution in ILs draw on the experience from cellulose. Since then, some ILs have been utilized as the innovative class of solvents in this process,[3, 31-33] including those with chloride, formate and acetate as anions, and 1-butyl-3-methylimidazolium ([Bmim]), 1-allyl-3-methylimidazolium ([Amim]), 1,3-dimethylimidazolium ([Dmim]) and 1-hydrogen-3-methylimidazolium ([Mim]) as cations. Moreover, the mixtures of ILs have also developed for the dissolution of chitosan.

Investigations on chitosan dissolution in ILs have shown that the anion of ILs had major influences on the solubility of chitosan. However, very few studies have been performed to explore the effects of cationic structure on the biopolymer dissolution,[34-36] and the deep mechanism of this process has not been well understood so far.

In this work, we mainly investigated some relative issues about dissolving chitosan into ILs. The ILs screened in this study are listed in Table S1, including a series of acetate-based aprotic ILs (AILs) [Emim]OAc, [Bmim]OAc, [Hmim]OAc, [Omim]OAc, [Bmmim]OAc, and [TEA]OAc, and protic ILs (PILs), [DEA]OAc, [BMOEA]OAc, and [Pyrrol]OAc. The solubilities of chitosan in these ILs have been measured as a function of temperature. The fixed anion $OAc^-$ with varied cation structures allowed us to examine the effect of the cation structure of ILs on the solubility of chitosan, as well as the related dissolution mechanism. The cationic core and structure, temperature and water content in the process of chitosan dissolution were also investigated. Most importantly, in order to reveal the interactions between the ILs and chitosan, temperature dependence of $^{13}C$ NMR spectra and density functional theory (DFT) computations were performed, which indicated that the interaction between cations and anions of ILs may be weaker and both cations and $OAc^-$ anion of ILs play significant roles in the dissolution process of chitosan by the disruption of inherent hydrogen bonds of chitosan.

## Experimental Section

### Materials

Chitosan with a stated deacetylation degree of 80.0-95.0% was purchased from Sinopharm Chem. Reagent Co. Ltd, and dried at 150 °C under vacuum before dissolution. The average molecular weight of the native chitosan is $2.59 \times 10^5$ Da, which can be obtained by measuring the intrinsic viscosity of chitosan/HAc/NaAc solution using an Ubbelodhe viscometer. The AILs used in the experiment were purchased from Lanzhou Greenchem ILs, LICP, CAS, China (Lanzhou, China) with purity over 99.9 %. The water contents of AILs were immediately determined by Karl-Fischer titration after drying them at 45 °C under vacuum conditions for 96 h and all of them were less than 1000 ppm. The method for preparing the PILs was followed according to the references.[37-39] Firstly, the starting reagents were purified, dried and handled under inert atmosphere. Then the equivalent value of neat Brønsted acids as well as Brønsted bases was added into a round-bottom flask simultaneously while stirred vigorously to dissipate the exothermic reaction heat. As confirmed by $^1H$ NMR and $^{13}C$ NMR (Bruker AM 400 MHz spectrometer), the prepared PILs samples are highly pure. The water contents of them were determined to be below 100 ppm by Karl-Fischer titration.

### Dissolution of chitosan in acetate-based ILs

The dried IL (about 5.0 g) was added in a 100 ml, 3-neck, round-bottom flask, which was then immersed in an oil bath (DF-101S, Henan Yuhua Instrument Factory). The temperature instability of the oil bath was estimated to be ± 1.0 °C. Under the continuous stirring, finely grinding chitosan powder (0.1 wt% of the IL) was added into the flask. Starting at 40 °C, this mixture was heated and stirred under nitrogen atmosphere. Additional chitosan (another 0.1 wt% of the IL) was added until the solution became clear, and we viewed the chitosan was saturated in the IL when the chitosan could not be dissolved under the certain temperature within 2 h. For each situation, the temperature was increased by 10 °C, up to the maximum temperature of 140 °C. The effect of water content (add quantitative water into neat IL) on chitosan solubility in [Bmim]OAc was also investigated.

### Measurement of solvatochromic parameters of the imidazolium-based ILs

The solvatochromic parameters were determined by the absorption peaks of the three dyes, N,N-diethyl-4-nitro-aniline (DENA), 4-nitroaniline (NA), and Reichardt's dye (RD) 33. The three kinds of stock solution were prepared by adding the dyes in methanol, then added 200μl to a quartz cuvette ($1 \times 0.1 \times 4.5$ cm) already contained ILs, and mixed homogeneously. The methanol was removed under vacuum at 40 °C for over 12h and then immediately measured through ultraviolet-visible (UV-vis) spectrophotometer (Carry5.0, Varian) at 20 °C for getting the $\lambda_{max}$.

### Measurements of $^{13}C$ NMR spectra at different temperature

$^{13}C$ NMR spectra measurements of the pure liquid [Bmim]OAc and the chitosan solution in [Bmim]OAc (8.0 wt% of chitosan) were performed on a Bruker DMX 300 spectrometer at different temperature. The solutions used here were prepared by adding the pure liquid [Bmim]OAc or the chitosan solution in [Bmim]OAc (8.0 wt% of chitosan) into a 5mm NMR tube, and then a capillary tube containing DMSO-$d_6$ was inserted to provide an external standard.

## Computational methods

Because a bundle of several chitosan chains, comprising dozens of chitobiose and interacting by intermolecular hydrogen bonding, are a very large system for DFT calculations, chitobiose was chosen as a model for the assessment of the electronic nature of the hydrogen bond and its chemical environment. Geometries of [Bmim]OAc and chitobiose were fully optimized at B3LYP/6-311++G (d,p) basis set. The chosen basis set contains diffuse functions that were required for the correct description of intramolecular hydrogen bonds.[40] The interaction energy (ΔE) including the basis set superposition errors (BSSE) correction using the counterpoise (CP) method was estimated. All the DFT calculations were carried out with Gaussian 03 package.[41]

## Results and Discussion

### The dissolution of chitosan in the imidazolium-based ILs

The solubility data of chitosan in imidazolium-based ILs investigated are summarized in Table 1. Among them, [Bmmim]OAc is white solid powder in the low temperature and called "ionic solid", so chitosan cannot be dissolved in the low temperature range. It shows that solubility of chitosan at a given temperature generally follows the orders: [Bmim]OAc > [Emim]OAc; [Bmim]OAc > [Hmim]OAc > [Omim]OAc; and [Bmim]OAc > [Bmmim]OAc. [Bmim]OAc is the most efficient IL for the chitosan dissolution. For these imidazolium-based ILs

with $OAc^-$ anion, the ILs with a shorter alkyl chain length have a larger ability of dissolving chitosan than those with a longer alkyl chain length.

On the basis of the chitosan solubility data, the standard solution Gibbs energy ($\Delta G_S^\theta$) for chitosan in the imidazolium-based ILs can be obtained by the following equation:

**Table 1** Solubilities of chitosan in the acetate-based ILs at different temperature

| | | | Solubility (gram per 100 g of the IL) | | | | | | | | | | |
|---|---|---|---|---|---|---|---|---|---|---|---|---|---|
| No. | Ionic Liquid | atmosphere | 40°C | 50°C | 60°C | 70°C | 80°C | 90°C | 100°C | 110°C | 120°C | 130°C | 140°C |
| 1 | [Emim]OAc | $N_2$ | -- | -- | 0.6 | 1.4 | 3.9 | 5.2 | 8.0 | 9.4 | 11.2 | 12.4 | 13.8 |
| 2 | [Bmim]OAc | $N_2$ | -- | 0.1 | 0.9 | 1.7 | 4.4 | 6.8 | 8.7 | 9.8 | 11.6 | 13.4 | >15.0 |
| 3 | [Hmim]OAc | $N_2$ | -- | -- | 0.6 | 1.4 | 2.7 | 3.6 | 5.2 | 6.8 | 7.8 | 9.2 | 12.0 |
| 4 | [Omim]OAc | $N_2$ | -- | -- | -- | 0.2 | 0.4 | 0.6 | 0.8 | 1.4 | 3.6 | 5.2 | 7.4 |
| 5 | [Bmmim]OAc[a] | $N_2$ | -- | -- | -- | -- | -- | -- | -- | -- | 6.4 | 8.2 | >9.8 |
| 6 | [TEA]OAc | $N_2$ | -- | -- | -- | -- | -- | -- | -- | -- | -- | 0.4 | 0.8 |
| 7 | [DEA]OAc | $N_2$ | -- | -- | -- | -- | -- | -- | -- | -- | -- | -- | -- |
| 8 | [DMOMA]OAc | $N_2$ | -- | -- | -- | -- | -- | -- | 0.5 | 0.9 | 1.7 | 2.6 | >3.6 |
| 9 | [Pyrrol]OAc | $N_2$ | -- | -- | -- | -- | -- | -- | 0.1 | 0.3 | 0.5 | 0.9 | 1.3 |

$$\Delta G_S^\theta = -RT \ln x \qquad (1)$$

where T stands for temperature, and x stands for the solubility of chitosan expressed by the mole fraction. It has been shown in Fig. 1 that the linear correlation can be observed in all the cases for the plots of ln x versus temperature. The standard solution enthalpy ($\Delta H_S^\theta$) can be obtained by equation 2 according to the Gibbs-Helmholtz equation and eq 1:[42]

$$\Delta H_S^\theta = RT^2\left(\frac{d \ln x}{dT}\right) \qquad (2)$$

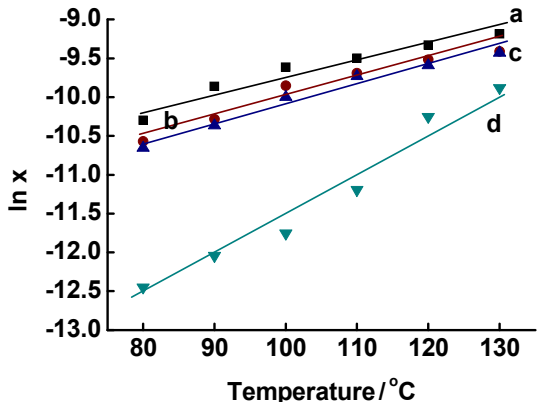


**Fig.** 1 Plots of ln x versus temperature for chitosan in [Bmim]OAc (a), [Emim]OAc (b), [Hmim]OAc (c) and [Omim]OAc (d), where x stands for the mole fraction of chitosan in ILs.

And the standard solution entropy ($T\Delta S_S^\theta$) can be obtained by

$$T\Delta S_S^\theta = \Delta H_S^\theta - \Delta G_S^\theta \qquad (3)$$

The thermodynamic parameters obtained are listed in Table S2. The $\Delta G_S^\theta$ values are positive for all the present systems, which suggests that the interation between the cations and anions may be stronger than that between chitosan and ILs, and the process of chitosan dissolution is unfavorable thermodynamically.[43] In the meantime, the positive $\Delta H_S^\theta$ and $\Delta S_S^\theta$ values for [Omim]OAc at whole temperature range and other imidazolium-based ILs at high temperature indicate that the chitosan dissolution in these processes is entropy driven, while it has no driven force since the $\Delta S_S^\theta$ values are negative for the ILs with short alkyl chain cations at the relative low temperature. As these processes are all non-spontaneous, the increase of temperature is necessary in order to enhance the dissolution of chitosan in the imidazolium-based ILs.

There is an approximate linear correlation between solubilities of chitosan at some given temperatures and the $^1H$ NMR chemical shifts of the proton in the 2-position of the imidazolium ring, which have an inseparable relationship with the anions of ILs. The strong hydrogen-bonding network of the polymer chains must be disrupted to dissolve these polysaccharides.[25] We know the anionic structure plays a key role in the disruption of the hydrogen bonds in chitosan, and $OAc^-$ anion is a strong hydrogen bond acceptor, but the role of cation of ILs in chitosan dissolution has been neglected and underestimated for a long time. Computational studies on the mechanism of polysaccharides dissolution in ILs have highlighted the interaction between the cation and cellulose *van der Waals* forces such as dispersive forces.[44] So, some intrinsic properties of imidazolium-based ILs with different cations and external factors do affect the solubilizing of chitosan.

The interactions between ILs and solute can be described by three solvatochromic parameters: the general dipolarity/polarizability (π*), the hydrogen bond acidity (α), and the hydrogen bond basicity (β). It is known that the β values can be used as a measure of the hydrogen bond accepting ability of anions of ILs; and the stronger hydrogen bond accepting ability the anion has, the greater the solubility of chitosan is.[3] Considering the fact that all of the ILs investigated in this study share the same anion but have different cations, we tried to find out the relationship between the solubility of chitosan and the other solvatochromic parameters. Table 2 summarizes the results obtained using solvatochromic UV-vis probe and the determined wavelengths of three dyes at the maximum absorption to calculate the solvatochromic parameters by the following equations: [26, 45-49]

$$\pi^* = 0.314(27.52 - \nu_{(DENA)}) \quad (4)$$

$$\nu_{(Dye)} = 1/(\lambda_{(Dye)max} \times 10^{-4}) \quad (5)$$

$$\beta = (1.035\nu_{(DENA)} + 2.64 - \nu_{(NA)})/2.80 \quad (6)$$

**Table 2** Solvatochromic parameters of imidazolium-based ILs used at 25°C.

| Entry. | Ionic Liquid | Added water content/ppm | Kamlet-Taft Parameters of Ionic Liquids | | | | | |
|---|---|---|---|---|---|---|---|---|
| | | | $E_T(33)$ | $E_T(30)$ | π* | α | β | β-α |
| 1 | [Emim]OAc | 0 | 57.38 | 48.52 | 0.869 | 0.493 | 1.154 | 0.661 |
| 2 | [Bmim]OAc | 0 | 53.15 | 44.66 | 0.970 | 0.470 | 1.156 | 0.686 |
| 3 | [Hmim]OAc | 0 | 56.00 | 47.24 | 0.801 | 0.462 | 1.152 | 0.690 |
| 4 | [Omim]OAc | 0 | 57.70 | 48.93 | 0.847 | 0.536 | 1.148 | 0.612 |
| 5 | [Bmim]OAc | 1060 | 58.25 | 49.31 | 0.924 | 0.505 | 1.096 | 0.591 |
| 6 | [Bmim]OAc | 5300 | 60.56 | 51.42 | 0.882 | 0.672 | 1.083 | 0.411 |
| 7 | [Bmim]OAc | 10540 | 61.63 | 52.40 | 0.907 | 0.718 | 1.054 | 0.336 |
| 8 | [Bmim]OAc | 50000 | 63.36 | 53.98 | 0.982 | 0.766 | 0.812 | 0.046 |

$$\alpha = 0.0649E_T(30) - 2.03 - 0.72\pi^* \quad (7)$$

$$E_T(30) = 0.9986E_T(33) - 8.6878 \quad (8)$$

$$E_T(33) = 28592/\lambda_{(RD33)max} \quad (9)$$

It indicates that the β values of these ILs with a fixed acetate anion are almost identical, but a slightly decreasing or resembled α values was found with the increasing chain length of the alkyl substituent on imidazolium ring,[50] which may be considered to estimate the ability of chitosan dissolution. Consequently, a combined parameter, the "net basicity" (β-α),[26] was calculated herein. Fig. 2 shows the relationship between the solubility of chitosan at 80 °C and the (β-α) parameter of the imidazolium-based ILs. It can be seen that solubility values of chitosan increase generally with the increase of (β-α) value of the ILs. In other words, IL with a greater β value and a smaller α value (a greater net basicity value) can dissolve more chitosan. Besides the formation of hydrogen bonds between the proton H on the –OH or $–NH_2$ groups of chitosan and the oxygen O of anions of the ILs, the hydrogen at C2 sites in the imidazolium cations can also interact with the residual of chitosan via hydrogen bonds, so the ILs with greater net basicity can dramatically disrupt the inter- and intra-molecular hydrogen bonds in chitosan and leads to the increase of solubility of chitosan.

Since the acetate-based ILs have high hydrophilicity and water content in ILs remarkably influences biomass solubility,[51-52] the influence of water on the ILs during dissolving chitosan was investigated systemmatically. Table S3 summarizes the results of different [Bmim]OAc/water systems. It can be shown that the solubility of chitosan in these systems decreases with increasing water content at a given temperature below 110°C, and the values are resemble when the temperature is higher. This suggests that water has been already evaporated when the solution is continuous stirred at a high temperature. The increasing of water content in chitosan-[Bmim]OAc decreases solution viscosity, but the stronger interaction between IL and water[51] can modify the diffusivity of the cation and anion of IL.[53] It can be concluded that water can form strong O-H-O hydrogen bonds with $OAc^-$ and weak C-H-O hydrogen bonds with cations, which indicates preferential solvation of anions by the adding of water.[54] It results in the weaken interaction between anions and chitosan. That is to say, the presence of water can significantly decrease the solubility of chitosan due to competitive hydrogen bonds to the chitosan microfibrils. So water in this system exists as an anti-solvent. For example, solubility of chitosan in [Bmim]OAc with no added water is neatly two times that with about 10000 ppm water at 80 °C. Particularly, chitosan almost cannot be dissolved when the water is over 50000 ppm in ILs.

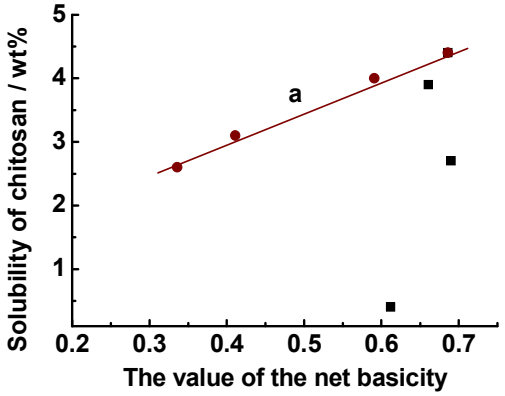


**Fig. 2** The linear correlation between solubility of chitosan at 80 °C and (β-α) parameter (the net basicity) of some system. The line a is for [Bmim]OAc with different water content. The other scatters are for 4 kinds of imidazolium-based ILs.

Then, the solvatochromic parameters were also assessed as a

function of the water content. Water has a low hydrogen bond basicity, but a high hydrogen bond acidity.[26] The solvatochromic parameters of the IL/water mixtures were measured by the same method above and the results are also summarized in Table 2. It has to be noted that α and β values are sensitive to water, and the β values decrease when adding water, while α values increase. In general, the growth of adding water content have caused continuous decline in (β-α) values of the IL/water mixtures, which is also verified that the ability of dissolving chitosan in IL may become weaker even at a low water content around 2000 ppm.

As depicted in Fig. 2, an approximate linear relationship is also given between the net basicity values of the IL/water mixtures and the solubility of chitosan at 80 °C. It indicates that the presence of water can make the net basicity values become smaller, leading to the decrease of dissolving chitosan. Besides, since these ILs are extremely hygroscopic, the water absorption from the humid air thus has significant influence not only on solvent viscosity but also on the solvation property of the mixture. Chitosan and ILs must be dried before using and the dry atmosphere needs to be applied in the dissolution experiment.

It can be obviously demonstrated that the solubility of chitosan in these imidazolium-based ILs increases with increasing temperature, and there is no doubt that the temperature plays a vital role in the procedure of dissolution. The relatively high temperature can enhance the solubility of chitosan due to aid in the evaporation of residual water from the ILs, which acts as an anti-solvent during the process of chitosan dissolution, and may change some transport properties of ILs at the same time. The values of viscosity were measured on an automated microviscometer by Anton Paar (AMVn). Fig. S1 shows the temperature dependency of density for imidazolium-based ILs. The density values decrease linearly with increasing temperature. The slope of the density in these ILs is approximately independent of the chain length of cation in the studied temperature range.

Fig. S2 gives the dynamic viscosity of the imidazolium-based ILs with temperature at the angle of 70 degree. The viscosities of the ILs used are obviously changed with the rising temperature. For every IL, only by heating up the sample by 10 °C, the viscosity reduces to approximately half, which can be also demonstrated that the ability of chitosan dissolution becomes greater as the temperature rising. Fig. S2 also shows the influence of alkyl chain length in imidazolium-based ILs with [OAc] anion on the viscosity. The viscosity value is greater for the ILs with a longer alkylchain length, *i.e.*, [Omim]OAc > [Hmim]OAc > [Bmim]OAc > [Emim]OAc. The ILs with greater viscosity value are not effective solvent for dissolution of chitosan due to the stronger interaction between the cations and anions. The effect of temperature on viscosity becomes weaker at higher temperature, but the ability of dissolving chitosan continues to increase. It indicates that viscosity is not the main factor for chitosan dissolution at high temperature. Moreover, the nonpolar alkyl cationic tail groups of ILs can aggregate when they are long enough, and then these ILs may form nanoscale spatial heterogeneity. The domain formation of tail groups on the cations resultsin a liquid crystal-like structure,[55-56] which can be also used to explain the weaker dissolution ability of the ILs with longer alkyl chains except for the steric effect on the interaction between the imidazolium ring and chitosan. Maybe the properties of ILs can be greatly changed, including their relative solvation potential. Therefore, the imidazolium-based ILs with shorter cationic alkyl chain length is necessary and important for the design of ILs for biomass utilization.

**The dissolution mechanism of chitosan in [Bmim]OAc**

In order to further examine the dissolution mechanism, $^{13}$C NMR measurements of pure [Bmim]OAc and the solution of chitosan/[Bmim]OAc have been determined at different temperature, and the $^{13}$C NMR spectra at 100 °C, as an example, are shown in Fig. 3 and Fig. 4A.

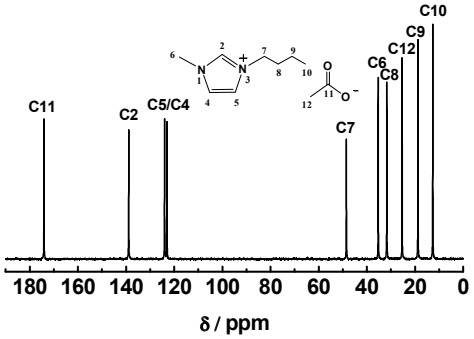


**Fig. 3** The $^{13}$C NMR spectra of pure [Bmim]OAc at 100 °C.

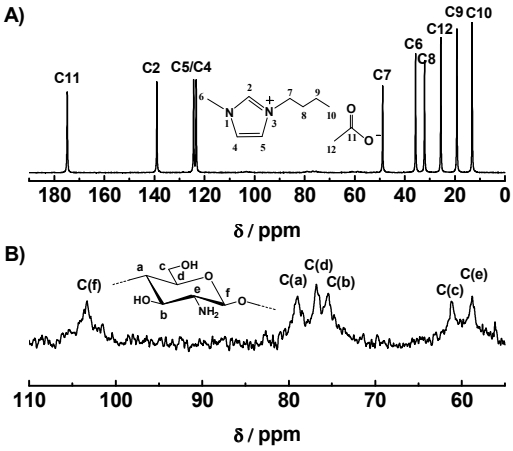


**Fig. 4** The $^{13}$C NMR spectra of 8.0 wt% chitosan in [Bmim]OAc solution at 100 °C. The signals are attributed to the carbon atoms on IL(A) and chitosan(B).

Since the high temperature can accelerate the molecular motion rate and weaken the intermolecular interaction between ions, the shielding effect is consequently decreasing with the increasing temperature. In the meantime, ion pair or hydrogen bonding of [Bmim]OAc may be dissociated significantly under high temperature, so the $^{13}$C NMR chemical shift per se may be affected by the change of temperature. Considering these factors, the NMR spectra of IL and mixture should be compared and analyzed at the same temperature. The detailed NMR data at several temperatures are given in Table 3. It can be seen that the dissolution of chitosan in [Bmim]OAc produces an upfield shift for every carbon atom except C11 at each temperature, while makes a downfield shift for C11. For the former, the upfield

chemical shift for the C2-C10 atoms and the C12 atom in $OAc^-$ can be possibly explained that the hydroxyl oxygen O and amino nitrogen N in chitosan may interact with the hydrogens in the $[Bmim]^+$ during the dissolution process. It leads to the increasing of the electron cloud density around the nine carbon atoms on the imidazolium ring. Likewise, the downfield shift for the C11 atom in anion indicates that a decrease of electron cloud density around this carbon atom and thus an increase of $^{13}C$ NMR signal. After that, we also found

Table 3 The relative $^{13}C$ NMR chemical shifts of the carbon atoms in [Bmim]OAc at different temperature. The values are obtained by the differences between the NMR chemical shifts of [Bmim]OAc in the solution of [Bmim]OAc with 8.0 wt% chitosan and the ones of pure [Bmim]OAc.

| | | The relative chemical shifts Δδ (ppm) of the carbon atoms in [Bmim]OAc | | | | | | | | | |
|---|---|---|---|---|---|---|---|---|---|---|---|
| | | 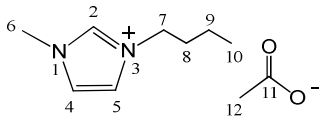 | | | | | | | | | |
| Entry | Temperature / °C | C2 | C4 | C5 | C6 | C7 | C8 | C9 | C10 | C11 | C12 |
| 1 | 25 | -0.13 | -0.10 | -0.12 | -0.11 | -0.10 | -0.09 | -0.08 | -0.10 | 0.14 | -0.12 |
| 2 | 40 | -0.15 | -0.11 | -0.12 | -0.13 | -0.11 | -0.12 | -0.09 | -0.13 | 0.16 | -0.13 |
| 3 | 60 | -0.18 | -0.14 | -0.14 | -0.13 | -0.13 | -0.14 | -0.11 | -0.16 | 0.20 | -0.16 |
| 4 | 80 | -0.22 | -0.16 | -0.18 | -0.16 | -0.14 | -0.15 | -0.13 | -0.17 | 0.23 | -0.18 |
| 5 | 100 | -0.25 | -0.20 | -0.21 | -0.18 | -0.17 | -0.17 | -0.16 | -0.19 | 0.26 | -0.19 |

from Table 3 that the decreasing extent of the chemical shift of C2 atom is obviously higher than the others, which implies that the C2 hydrogen has the strongest interaction with the hydroxyl oxygen O or amino nitrogen N in chitosan. These results are in agreement with the previous recognition of the stronger acidity and hydrogen donor ability of the C2 proton on the imidazolium ring. It can be concluded that both cation and anion play significant roles in the process of destroying the inter- and intra-molecular hydrogen bonds in chitosan. In addition, it is interesting to note that for each carbon atom in [Bmim]OAc, the relative chemical shifts Δδ increase with the increasing temperature. Due to the transformation of the diffusion particles in IL from ion pairs to individual ions at high temperature, more opportunities for ions can be created to interact with chitosan. As confirmed by the NMR experimental results, stronger interaction between cation-anion and chitosan may exist in the system, which is a possible explanation for solubility enhancement of chitosan in [Bmim]OAc at high temperature.

On the other hand, because of the low concentration of chitosan, the signals are relative weak in the $^{13}C$ NMR spectra. The six signals of the unmodified glucosamine unit appear clearly at 103.32, 78.97, 76.80, 75.43, 61.20 and 58.79 ppm in Fig. 4B, which are attributed to the C(f), C(a), C(d), C(b), C(c) and C(e) of chitosan, respectively. It is very similar to the spectrum of chitosan dissolved in other solvents such as acetic acid and the signals of the six kinds of carbon atoms are well-resolved. It can be concluded that [Bmim]OAc acts as a truly favorable solvent in the process of chitosan dissolution, in which chitosan could be well dispersed.

Furthermore, computational studies applying DFT have been also performed in order to uncover the mechanistic aspects of the chitosan dissolution in acetate-based ILs. Because of the limited computing power for biomacromolecule, chitobiose has been chosen as an excellent model for chitosan. Since the supermolecular structure of the chitosan constitutional unit is built up through side-by-side packing of the chains, both inermolecular hydrogen bond N-H-O and O-H-O may occur in the network, which traditional molecular solvents can only access the polymeric chains at the surface of chitosan. In an endeavor to understand the hydrogen bonds interactions among the chitobiose, we screened two kinds of hydrogen bond O-H-O to compare the interaction strength of [Bmim]OAc in the process of chitosan dissolution. One is formed by the interaction between the oxygen atoms in pyran ring and the substituent (O(R)-H-O(S)), which can be defined as the intrachain hydrogen bonds. And the other is the interaction between two oxygen atoms in the substituent (O(S)-H-O(S)), which can be defined as the interchain hydrogen bonds.

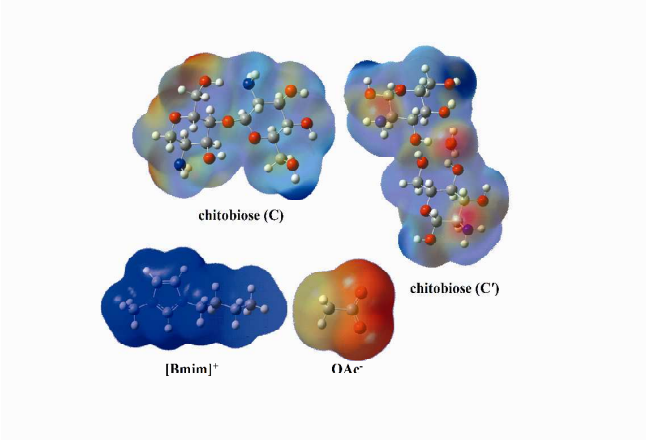


**Fig. 5** The electrostatic potential surfaces for chitobiose and the cation and anion of [Bmim]OAc optimized completely at B3LYP/6-311++G(d,p) basis set.

Fig.5 shows the electrostatic potential surfaces for chitobiose (C and C′ ) and the cation and anion of [Bmim]OAc, where the red colours and blue colours indicate the regions with more negative charges and positive charges, respectively. It is clear that the red region of $OAc^-$ is the most favourable sites for proton attack, and new hydrogen bonds can be formed between chitobiose and anions. For the chitobiose, the red region means the possible interaction with the cations of [Bmim]OAc. On the other hand, the blue region means the interaction of the proton H on the hydroxyl groups in chitobiose with the oxygen on the carboxyl group in $OAc^-$. It is entirely consistent with the NMR experiment results.

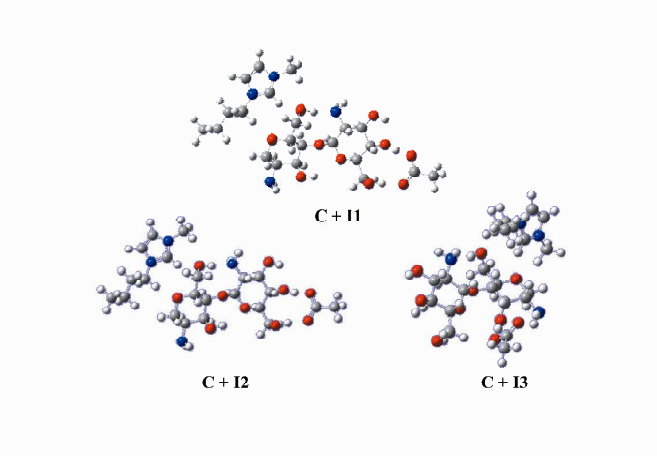


**Fig. 6** Optimized structures of different conformers **1-3** by the interaction between chitobiose (C) and [Bmim]OAc (I).

Different conformers (C+I1-3) formed by the interaction between chitobiose (C) and [Bmim]OAc were optimized and shown in Fig. 6. From the optimizd structures, we can found that the C2 hydrogen on the imidazolium ring may interact with the hydroxymethyl of chitobiose and $OAc^-$ anion linked to the hydroxyl in the pyran ring. In addition, water was used as a contrast to demonstrate the role of IL in the process of chitosan dissolution. The conformers (C+W1-5) were also optimized (Fig. 7). Fig. S3 shows the most stable geometries of the isolated ionic pair and chitobiose, chitobiose/$H_2O$ and chitobiose/[Bmim]OAc. For chitoboise/[Bmim]OAc system, we can observe these hydrogen bonds: O(5)-H(6) ⋯ O(1), O(4)-H(5) ⋯ O(1), O(4)-H(3) ⋯ O(6) and O(5)-H(4) ⋯ O(7). These intermolecular hydrogen bonds are expected to be an key factor resulting in the high solubility of chitosan in [Bmim]OAc. For the system of chitobiose/$H_2O$, the calculated H(5) ⋯ O(3) and H(3) ⋯ O(6) distance is 1.82 Å and 1.81 Å respectively ,which are both shorter than the summation (2.72 Å) of the *van der* Waals radii of O and H atoms, and the O(6)-H(5)⋯O3 angle is 170.42° and O(4)-H(3) ⋯O(6) angle is 169.93°. These data indicate the formation of O(6)-H(5)⋯O(3) and O(4)-H(3)⋯O(6) hydrogen bonds between the chitobiose and $H_2O$.

In the meantime, the energy variations (ΔE) in the dissolution process are also calculated, which can be shown the interaction strength between chitobiose and [Bmim]OAc or $H_2O$. It shows that interaction energy ΔE of three conformers between chitobiose (C) and [Bmim]OAc was -2043.99 kJ/mol, -2043.98 kJ/mol and -2025.85 kJ/mol, respectively. In the other hand, the highest interaction energy ΔE between chitobiose (C) and water was -146.07 kJ/mol, which was much less than that of [Bmim]OAc. It indicates that [Bmim]OAc has much stronger ability to disrupt intrachain hydrogen bonds of chitosan than that of water.

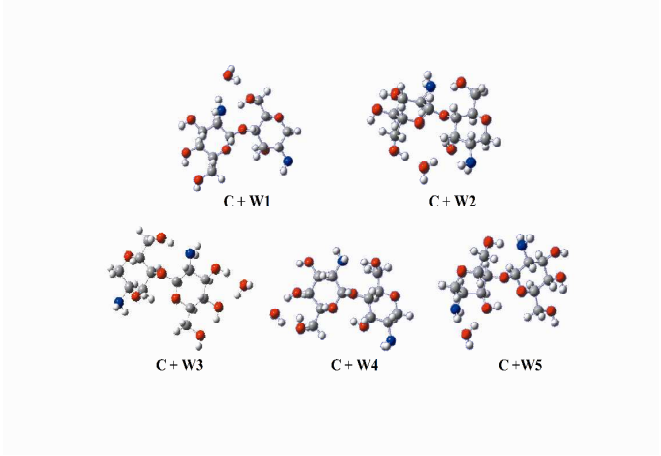


**Fig. 7** Optimized structures of different conformers **1-5** by the interaction between chitobiose (C) and water (W).

Fig. 8 shows the optimized structures of the chitobiose formed by the interchain hydrogen bonds interaction O(S)-H-O(S) and the conformers interacted by chitobiose (C′ ) and solvent. Similarly, we attempted to calculate the interaction energy ΔE of them. It was found that the ΔE value of (C′ + W) is 146.78 kJ/mol, which is approximately equal to that of (C + W), and the ΔE value of (C′ + I) is 400245.56 kJ/mol, which is much higher than that of (C + I). We can conclude that the interchain hydrogen bonds may be disrupted by cations and anions of IL prior to the intrachain hydrogen bonds in the process of chitosan dissolution.

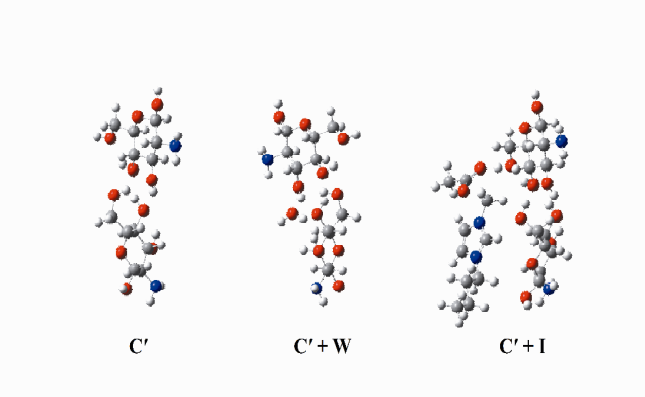


**Fig. 8** Optimized structures of chitobiose (C′) and conformers by the interaction between chitobiose (C′) and water (W) or [Bmim]OAc (I).

### The solubility of chitosan in thequaternary ammonium-based ILs

The solubility data of chitosan in the quaternary ammonium-based ILs are also given in Table 1. In all, the ILs with ammonium cations can only dissolve a very small amount of chitosan. This can be explained that in imidazolium-based ILs, the main interactions between cations and anions involve both coulombic force and hydrogen bonds.[57] When adding chitosan in imidazolium-based ILs, chitosan can be dissolved through both of interactions. For the [TEA]OAc lack of active hydrogen, the interactions between the cations and anions of ILs may only exist as the coulombic interaction. However, the hydrogen bonds may dominate, and both the anions and cations play important roles in the process of chitosan dissolution, leading to the low solubility in the quaternary ammonium-based ILs.

The order of chitosan solubility in the three kinds of PILs is: [BMOEA]OAc > [Pyrrol]OAc > [DEA]OAc. Numerous cases exist to illustrate the phenomenon. Firstly, the presence of the protic cations can distract the $OAc^-$ anion from forming hydrogen bond with chitosan oligomers. [BMOEA]OAc has oxygen containing functional group in their cations and the oxygen atom here can also act as hydrogen bond acceptor, which have been demonstrated that the ability of dissolution chitosan is a little more.[58-59] In addition, the ether oxygen atom only forms bonds with two atoms rather than four atoms for the carbon atom and a smaller atomic radius of the oxygen atom compared to a carbon atom as a result of lots of holes between ions may come into existence, so the lower viscosity of [BMOEA]OAc may reflect and more chitosan may be dissolved in.[60] Next, the steric hindrance makes a cyclic molecule be relatively harder to attack the solute. In short, the ability of chitosan dissolution in ILs is complicated, and it is the outcome of many factors co-action.

Comparatively, the ability of chitosan dissolution in the quaternary ammonium-based ILs is much weaker than that of imidazolium-based ones. The most key property that distinguish PILs from AILs is the proton can transfer from the Brønsted acid to the Brønsted base, leading to the presence of proton-donor and proton-acceptor sites, which can be used to build up a more unique hydrogen bond network.[61] In reality, the proton transfer from the acid to the base in PILs may be less than complete, resulting in the neutral species also being present except the ions.[62] Besides, in the system aggregation and association of either ions or molecules can occur. So a concept of ionicity for PILs must be concern about, and the equilibrium between the ionic and non-ionic forms and the aggregates make the ionicity of PILs more complex ascompared to AILs.[63-65] The ionicity of the present PILs can be explained using a strong hydrogen bond net between inter ionic interaction, which is too firm to attack the polymers hydrogen bond net. It can be demonstrated that solubility of chitosan in PILs used is less than 1/10 of that in [Bmim]OAc. The ionicity of PILs becomes lower at high temperature[63-64] due to the possibility of back proton transfer through an equilibrium shift toward neutral components and the successive breaking of hydrogen bonds with temperature. Likewise, solubility of chitosan increases with increasing temperature. However, dissolving chitosan in PILs under high temperature is still at a low level for two reasons. One is the formation of ion-aggregates or ion-clusters and they may have a relatively close structure, which are not suitable for dissolving process. The other is decomposition reaction may occur at the experimental temperature. These PILs containing the acetate anion, have lower thermal stability due to undergoing a condensation reaction to form amides.[66] For [DEA]OAc and [Pyrrol]OAc, we can detect the transgression of free ammonia when heating them. After the samples being cool, the colors and character change. For example, [DEA]OAc changes from the light yellow liquid to the darker solid. Thus, these PILs are not recyclable for chitosan dissolution.

## Conclusions

In summary, the systematic investigations on the solubilities of the high crystallization degree of chitosan in some acetate-based ILs and the possible interactions between chitosan and ILs have been carried out. It is found that for the present acetate-based ILs with the fixed anion $OAc^-$, the solubilities of chitosan measured as a function of temperature in the imidazolium-based ILs are much higher than those in the quaternary ammonium-based ILs, which indicates that although anionic structure plays a key role in the disruption of the hydrogen bonds in chitosan, the role of cation of ILs in chitosan dissolution cannot be neglected. Among them, [Bmim]OAc has the highest amount of chitosan dissolution of over 15.0 (gram per 100g of the IL) at 140 °C under $N_2$atmosphere.For the imidazolium-based ILs, the process of chitosan dissolution is non-spontaneous and thermodynamically unfavorable. The ability of dissolving chitosan in IL becomes weaker at low water content around 2000 ppm. It is also interesting to note that both cations and $OAc^-$ anion of ILs play significant roles in the dissolution process of chitosan possibly by the disruption of inherent hydrogen bonds of chitosan by using temperature dependence of $^{13}C$ NMR spectra and DFT computations. We can also conclude that the interchain hydrogen bonds may be disrupted by cations and anions of IL prior to the intrachain hydrogen bonds in the process of chitosan dissolution. The information obtained here may provide a guide for the design and synthese of new solvents for the treatment of chitosan or other biomass.

## Acknowledgements

This work was supported by the National Natural Science Foundation of China (21173267).

## Notes and references

[a] Department of Chemistry, Renmin University of China, Beijing 100872, P. R. China. Tel: 8610-62514925, Email : tcmu@chem.ruc.edu.cn
[b] School of Chemistry and Chemical Engineering, Qufu Normal University, Qufu 273165, P. R. China

† Electronic Supplementary Information (ESI) available: [details of any supplementary information available should be included here]. See DOI: 10.1039/b000000x/

1. K. Yao and C. Tang, *Macromolecules*, 2013, **46**, 1689-1712.
2. A. M. Dias, A. R. Cortez, M. Barsan, J. Santos, C. M. Brett and H. C. de Sousa, *ACS Sustain. Chem. Eng.*, 2013, **1**, 1480-1492.
3. Q. T. Chen, A. R. Xu, Z. Y. Li, J. J. Wang and S. J. Zhang, *Green Chem.*, 2011, **13**, 3446-3452.
4. E. Khor and L. Y. Lim, *Biomaterials*, 2003, **24**, 2339-2349.
5. M. Dash, F. Chiellini, R. Ottenbrite and E. Chiellini, *Prog. Polym. Sci.*, 2011, **36**, 981-1014.
6. M. N. Ravi Kumar, *React. Funct. Polym.*, 2000, **46**, 1-27.
7. A. Ayoub, R. A. Venditti, J. J. Pawlak, A. Salam and M. A. Hubbe, *ACS Sustain. Chem. Eng.*, 2013, **1**, 1102-1109.
8. M. Rinaudo, G. Pavlov and J. Desbrieres, *Polymer*, 1999, **40**, 7029-7032.
9. X. Geng, O.-H. Kwon and J. Jang, *Biomaterials*, 2005, **26**, 5427-5432.
10. H. Sashiwa, N. Kawasaki, A. Nakayama, E. Muraki and S.-i. Aiba, *Chitin Chitosan Res.*, 2002, **8**, 249-251.
11. M. Petkovic, K. R. Seddon, L. P. N. Rebelo and C. S. Pereira, *Chem. Soc. Rev.*, 2011, **40**, 1383-1403.
12. N. V. Plechkova and K. R. Seddon, *Chem. Soc. Rev.*, 2008, **37**, 123-150.
13. V. H. Jadhav, H. J. Jeong, S. T. Lim, M. H. Sohn and D. W. Kim, *Org. Lett.*, 2011, **13**, 2502-2505.
14. P. Wasserscheid and W. Keim, *Angew. Chem. Int. Ed.*, 2000, **39**, 3772-3789.
15. J. Dupont, R. F. de Souza and P. A. Z. Suarez, *Chem. Rev.*, 2002, **102**, 3667-3691.
16. Z. M. Zhou, Z. H. Li, X. Y. Hao, X. Dong, X. Li, L. Dai, Y. Q. Liu, J. Zhang, H. F. Huang, X. Lia and J. L. Wang, *Green Chem.*, 2011, **13**, 2963-2971.
17. J. Sun, J. Q. Wang, W. G. Cheng, J. X. Zhang, X. H. Li, S. J. Zhang and Y. B. She, *Green Chem.*, 2012, **14**, 654-660.
18. Z. Sun, M. X. Cheng, H. C. Li, T. Shi, M. J. Yuan, X. H. Wang and Z. J. Jiang, *RSC Adv.*, 2012, **2**, 9058-9065.
19. X. X. Zhang, W. Zhang, D. Tian, Z. H. Zhou and C. H. Lu, *RSC Adv.*, 2013, **3**, 7722-7725.
20. R. Vijayaraghavan, A. Izgorodin, V. Ganesh, M. Surianarayanan and D. R. MacFarlane, *Angew. Chem. Int. Ed.*, 2010, **49**, 1631-1633.
21. H. P. Steinruck, J. Libuda, P. Wasserscheid, T. Cremer, C. Kolbeck, M. Laurin, F. Maier, M. Sobota, P. S. Schulz and M. Stark, *Adv. Mater.*, 2011, **23**, 2571-2587.
22. Y. Q. Zhang, H. X. Gao, Y. H. Joo and J. M. Shreeve, *Angew. Chem. Int. Ed.*, 2011, **50**, 9554-9562.
23. R. P. Swatloski, S. K. Spear, J. D. Holbrey and R. D. Rogers, *J. Am. Chem. Soc.*, 2002, **124**, 4974-4975.
24. A. W. T. King, J. Asikkala, I. Mutikainen, P. Jarvi and I. Kilpelainen, *Angew. Chem. Int. Ed.*, 2011, **50**, 6301-6305.
25. C. Froschauer, M. Hummel, G. Laus, H. Schottenberger, H. Sixta, H. K. Weber and G. Zuckerstatter, *Biomacromolecules*, 2012, **13**, 1973-1980.
26. L. K. J. Hauru, M. Hummel, A. W. T. King, I. Kilpelainen and H. Sixta, *Biomacromolecules*, 2012, **13**, 2896-2905.
27. J. Vitz, T. Erdmenger, C. Haensch and U. S. Schubert, *Green Chem.*, 2009, **11**, 417-424.
28. A. R. Xu, J. J. Wang and H. Y. Wang, *Green Chem.*, 2010, **12**, 268-275.
29. B. Zhao, L. Greiner and W. Leitner, *RSC Adv.*, 2012, **2**, 2476-2479.
30. X. Sun, Y. Chi and T. Mu, *Green Chem.*, 2014, **16**, 2736-2744.
31. Y. Wu, T. Sasaki, S. Irie and K. Sakurai, *Polymer*, 2008, **49**, 2321-2327.
32. W. Xiao, Q. Chen, Y. Wu, T. Wu and L. Dai, *Carbohydr. Polym.*, 2011, **83**, 233-238.
33. X. Sun, Z. Xue and T. Mu, *Green Chem.*, 2014, **16**, 2102-2106.
34. R. C. Remsing, I. D. Petrik, Z. Liu and G. Moyna, *Phys. Chem. Chem. Phys.*, 2010, **12**, 14827-14828.
35. J. Zhang, H. Zhang, J. Wu, J. Zhang, J. He and J. Xiang, *Phys. Chem. Chem. Phys.*, 2010, **12**, 14829-14830.
36. Y. Zhao, X. Liu, J. Wang and S. Zhang, *ChemPhysChem*, 2012, **13**, 3126-3133.
37. C. Zhao, A. M. Bond and X. Y. Lu, *Anal. Chem.*, 2012, **84**, 2784-2791.
38. C. Zhao, G. Burrell, A. A. J. Torriero, F. Separovic, N. F. Dunlop, D. R. MacFarlane and A. M. Bond, *J. Phys. Chem. B*, 2008, **112**, 6923-6936.
39. G. L. Burrell, I. M. Burgar, F. Separovic and N. F. Dunlop, *Phys. Chem. Chem. Phys.*, 2010, **12**, 1571-1577.
40. G. I. Csonka, A. D. French, G. P. Johnson and C. A. Stortz, *J. Chem. Theory Comput.*, 2009, **5**, 679-692.
41. M. J. Frisch, G. W. Trucks, H. B. Schlegel, G. E. Scuseria, M. A. Robb, J. R. Cheeseman, J. A. Montgomery, T. Vreven, K. N. Kudin, J. C. Burant, J. M. Millam, S. S. Iyengar, J. Tomasi, V. Barone, B. Mennucci, M. Cossi, G. Scalmani, N. Rega, G. A. Petersson, H. Nakatsuji, M. Hada, M. Ehara, K. Toyota, R. Fukuda, J. Hasegawa, M. Ishida, T. Nakajima, Y. Honda, O. Kitao, H. Nakai, M. Klene, X. Li, J. E. Knox, H. P. Hratchian, J. B. Cross, V. Bakken, C. Adamo, J. Jaramillo, R. Gomperts, R. E. Stratmann,O. Yazyev, A. J. Austin, R. Cammi, C. Pomelli, J. W. Ochterski, P. Y. Ayala, K. Morokuma, G. A. Voth, P. Salvador, J. J. Dannenberg, V. G. Zakrzewski, S. Dapprich, A. D. Daniels, M. C. Strain, O. Farkas, D. K. Malick, A. D. Rabuck, K. Raghavachari, J. B. Foresman, J. V. Ortiz, Q. Cui, A. G. Baboul, S. Clifford, J. Cioslowski, B. B. Stefanov, G. Liu, A. Liashenko, P. Piskorz, I. Komaromi, R. L. Martin, D. J. Fox, T. Keith, Al M. A. Laham, C. Y. Peng, A. Nanayakkara, M. Challacombe, P. M. W. Gill, B. Johnson, W. Chen, M. W. Wong, C. Gonzalez, J. A. Pople, Gaussian 03, revision C.02; Gaussian, Inc.: Wallingford, CT, **2004**.
42. A. J. Queimada, F. L. Mota, S. P. Pinho and E. A. Macedo, *J. Phys. Chem. B*, 2009, **113**, 3469-3476.
43. Y. Zheng, X. Xuan, J. Wang and M. Fan, *J. Phys. Chem. A*, 2009, **114**, 3926-3931.
44. H. M. Cho, A. S. Gross and J. W. Chu, *J. Am. Chem. Soc.*, 2011, **133**, 14033-14041.
45. C. Reichardt, *Green Chem.*, 2005, **7**, 339-351.
46. R. Lungwitz and S. Spange, *New J. Chem.*, 2008, **32**, 392-394.
47. A. Oehlke, K. Hofmann and S. Spange, *New J. Chem.*, 2006, **30**, 533-536.
48. Y. Fukaya, A. Sugimoto and H. Ohno, *Biomacromolecules*, 2006, **7**, 3295-3297.
49. S. K. Shukla, N. D. Khupse and A. Kumar, *Phys. Chem. Chem. Phys.*, 2012, **14**, 2754-2761.
50. M. Ab Rani, A. Brant, L. Crowhurst, A. Dolan, M. Lui, N. Hassan, J. Hallett, P. Hunt, H. Niedermeyer and J. Perez-Arlandis, *Phys. Chem. Chem. Phys.*, 2011, **13**, 16831-16840.
51. L. E. Ficke and J. F. Brennecke, *J. Phys. Chem. B*, 2010, **114**, 10496-10501.
52. Y. Y. Cao, Y. Chen, X. F. Sun, Z. M. Zhang and T. C. Mu, *Phys. Chem. Chem. Phys.*, 2012, **14**, 12252-12262.
53. K. A. Le, R. Sescousse and T. Budtova, *Cellulose*, 2012, **19**, 45-54.
54. Y. L. Zhao, X. M. Liu, J. J. Wang and S. J. Zhang, *J. Phys. Chem. B*, 2013, **117**, 9042-9049.
55. Y. T. Wang, *J. Phys. Chem. B*, 2009, **113**, 11058-11060.
56. Y. T. Wang and G. A. Voth, *J. Am. Chem. Soc.*, 2005, **127**, 12192-12193.
57. S. Zhang, Z. Chen, X. Qi and Y. Deng, *New J. Chem.*, 2012, **36**, 1043-1050.
58. S. K. Tang, G. A. Baker, S. Ravula, J. E. Jones and H. Zhao, *Green Chem.*, 2012, **14**, 2922-2932.

59. H. Zhao, G. A. Baker, Z. Y. Song, O. Olubajo, T. Crittle and D. Peters, *Green Chem.*, 2008, **10**, 696-705.
60. Z. J. Chen, T. Xue and J.-M. Lee, *RSC Adv.*, 2012, **2**, 10564-10574.
61. T. L. Greaves and C. J. Drummond, *Chem. Rev.*, 2008, **108**, 206-237.
62. X. Sun, S. Liu, A. Khan, C. Zhao, C. Yan and T. Mu, *New J. Chem.*, 2014, DOI: 10.1039/c4nj00384e.
63. M. S. Miran, H. Kinoshita, T. Yasuda, M. Abu Bin, H. Susanz and M. Watanabe, *Chem. Commun.*, 2011, **47**, 12676-12678.
64. M. S. Miran, H. Kinoshita, T. Yasuda, M. A. Susan and M. Watanabe, *Physical Chemistry Chemical Physics*, 2012, **14**, 5178-5186.
65. K. Ueno, H. Tokuda and M. Watanabe, *Phys. Chem. Chem. Phys.*, 2010, **12**, 1649-1658.
66. T. L. Greaves, A. Weerawardena, C. Fong, I. Krodkiewska and C. J. Drummond, *J. Phys. Chem. B*, 2006, **110**, 22479-22487.

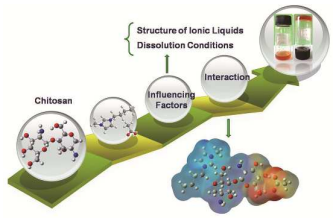


Herein, both experimental evidence and density functional theory analysis are used to explore the interactions between IL and chitosan.